

Forgetting-Resistant and Lesion-Aware Source-Free Domain Adaptive Fundus Image Analysis with Vision-Language Model

Zheang Huai, Hui Tang, Hualiang Wang, and Xiaomeng Li

The Hong Kong University of Science and Technology, Kowloon, Hong Kong

Abstract. Source-free domain adaptation (SFDA) aims to adapt a model trained in the source domain to perform well in the target domain, with only unlabeled target domain data and the source model. Taking into account that conventional SFDA methods are inevitably error-prone under domain shift, recently greater attention has been directed to SFDA assisted with off-the-shelf foundation models, e.g., vision-language (ViL) models. However, existing works of leveraging ViL models for SFDA confront two issues: (i) Although mutual information is exploited to consider the joint distribution between the predictions of ViL model and the target model, we argue that the forgetting of some superior predictions of the target model still occurs, as indicated by the decline of the accuracies of certain classes during adaptation; (ii) Prior research disregards the rich, fine-grained knowledge embedded in the ViL model, which offers detailed grounding for fundus image diagnosis. In this paper, we introduce a novel forgetting-resistant and lesion-aware (FRLA) method for SFDA of fundus image diagnosis with ViL model. Specifically, a forgetting-resistant adaptation module explicitly preserves the confident predictions of the target model, and a lesion-aware adaptation module yields patch-wise predictions from ViL model and employs them to help the target model be aware of the lesion areas and leverage the ViL model’s fine-grained knowledge. Extensive experiments show that our method not only significantly outperforms the vision-language model, but also achieves consistent improvements over the state-of-the-art methods. Our code will be released.

Keywords: Source-free domain adaptation · Vision-language model · Patch-wise supervision · Mutual information.

1 Introduction

Fundus photography plays a vital role in screening retinal diseases, which can result in vision impairment or blindness if left untreated [20]. While deep neural networks have demonstrated excellent performance in fundus image diagnosis [11], they are susceptible to domain shifts caused by variations in imaging protocols or scanning devices [21, 31]. Source-free domain adaptation (SFDA) has been introduced to address the domain shift problem by adapting a model

pre-trained with source-domain images to adapt to the target domain distribution without any target domain annotation. SFDA has become a significant research focus [10, 14, 22–24, 27], as it eliminates the need to access the source data during domain adaptation, thereby ensuring the privacy of sensitive data.

Traditional solutions to SFDA for classification conduct pseudo-labeling based self-training [3, 9, 12, 15], exploit local feature structure under domain shift [25, 26], or harness self-supervised contrastive learning to facilitate target domain feature learning [4, 8, 29]. Most recently, inspired by the rich and heterogeneous knowledge held by foundation models, more efforts have been paid to SFDA aided by foundation models. Co-learn [28] integrates the pre-trained network, e.g. Swin Transformer [13], into the target domain adaptation, to leverage the alternate view of features and classifications different from source model. DIFO [19] employs the frozen vision-language (ViL) model, e.g. CLIP [16], and alternates between customizing CLIP through prompt learning and distilling the knowledge of CLIP to the target model, exhibiting a higher performance than Co-learn.

In this paper, we build upon the line of SFDA research that utilizes the ViL model. We identify and solve two main limitations of existing methods. First, mutual information (MI) loss has been proved in [19] to be highly effective for distilling valuable ViL model knowledge in SFDA, as it takes into account the joint distribution between the predictions of ViL model and the target model. However, we observe that the forgetting of some high-quality predictions of the target model still happens. In other words, certain superior predictions made by the target model are influenced negatively by the ViL model (see the first two rows in Table 2 for the drop in the accuracies of certain classes after adaptation). Second, current works [19, 28] only make use of the global image-level information provided by foundation models, neglecting the fine-grained and more informative knowledge, such as patch-wise predictions, that foundation models can offer. Such detailed knowledge is beneficial for the adaptation of a fundus image diagnosis model by informing it of the locations of lesions in fundus images, e.g. exudates, drusen, and abnormal optic cup [5].

To tackle the aforementioned issues, we present an innovative forgetting-resistant and lesion-aware (FRLA) method for SFDA of fundus image diagnosis with ViL model. First, after each period of adaptation, a *forgetting-resistant adaptation* module calculates the up-to-date predictions from the target model and stores them in a memory bank. When distilling ViL model knowledge via MI loss, reliable predictions in the memory bank are selected and explicitly preserved by an introduced additional MI loss term between target model’s predictions and the selected predictions. In addition, a *lesion-aware adaptation* module is devised to obtain patch-wise predictions of the ViL model and adaptively exert patch-level supervision, enabling the target model to be aware of lesion areas during training. Extensive experiments conducted on two pairs of cross-domain multi-disease fundus image datasets indicate that our proposed approach not only significantly surpasses the vision-language model, but also yields superior performance compared to the state-of-the-art methods [9, 12, 19, 28].

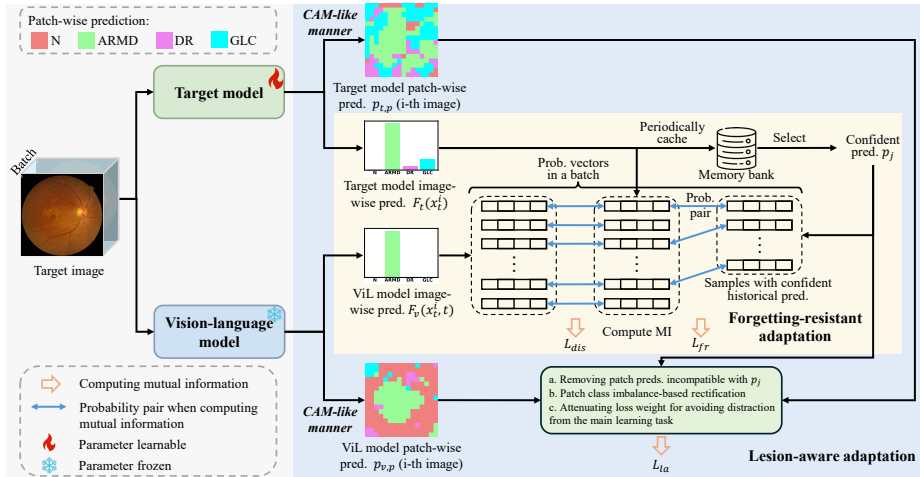


Fig. 1. The framework of our proposed FRLA, which comprises forgetting-resistant adaptation and lesion-aware adaptation. The meanings of the disease abbreviations are given in Sec. 3. The text input of ViL model is omitted for simplicity.

2 Method

Problem Formulation. In the SFDA problem, a source model $F_s : \mathcal{X}_s \rightarrow \mathcal{Y}_s$ is trained using the data $\{x_s^i, y_s^i\}_{i=1}^{n_s}$ from the source domain \mathcal{D}_s with a supervision loss such as cross-entropy. $\mathcal{D}_s = (\mathcal{X}_s, \mathcal{Y}_s)$, where $(x_s^i, y_s^i) \in (\mathcal{X}_s, \mathcal{Y}_s)$. Also an unlabeled dataset $\{x_t^i\}_{i=1}^{n_t}$ from the target domain \mathcal{D}_t is given, where $x_t^i \in \mathcal{D}_t$. The source and target domains are assumed to share the same K classes. We aim to learn a target model $F_t : \mathcal{X}_t \rightarrow \mathcal{Y}_t$ with (1) the source model F_s , (2) the unlabeled target dataset $\{x_t^i\}_{i=1}^{n_t}$, and (3) a vision-language (ViL) foundation model denoted as F_v . In our experiments, the foundation model we adopt is FLAIR [17], a reputable ViL model for fundus images. Nonetheless, our method can be extended to other fundus ViL models.

Overview. Fig. 1 illustrates our forgetting-resistant and lesion-aware (FRLA) framework for SFDA. In this section, we first introduce the forgetting-resistant adaptation that explicitly maintains the portion of the superior predictions of the target model in the process of the interaction between the target model and ViL model. Next, we propose the lesion-aware adaptation strategy which employs the fine-grained supervision from ViL model to make the fundus image diagnosis model aware of the lesion regions while adapting to the target domain.

2.1 Forgetting-Resistant Adaptation with Dual Mutual Information Loss

In the scenario of SFDA, mutual information is demonstrated to be the optimal loss choice when distilling the knowledge of ViL model to the target model [19],

as mutual information captures the joint distributions between the target model predictions and ViL model predictions. As analyzed both theoretically and empirically in [19], mutual information considers the correlation between the two model predictions, rather than exhibits a bias towards a specific model. Nevertheless, we observe in our experiments that certain correct and highly confident predictions of the target model might still be affected negatively during training.

To address this challenge, we propose to periodically perform inference on the target domain data using the target model that is initialized with the source model, and store the predicted results in a memory bank. During adaptation, the confident predictions in the memory bank are selected to form an additional mutual information loss with the target model output.

Formally, for a batch of B target domain images $\{x_t^i\}_{i=1}^B$, we first follow [19] to maximize the mutual information between the target model predictions and ViL model predictions as

$$\mathcal{L}_{dis} = -\text{MI}(F_t(x_t^i)_{i=1}^B, F_v(x_t^i, t)_{i=1}^B), \quad (1)$$

where $\text{MI}(\cdot, \cdot)$ denotes mutual information, and t is the text prompts formatted as in [17]. Let p_i be the probabilities stored in the memory bank corresponding to this batch of samples. We first compare their confidence $\text{Max}(p_i)$ with a threshold τ to select B' confident samples, whose stored probabilities are represented as $\{p_j\}_{j=1}^{B'}$. Then the forgetting-resistant adaptation loss is proposed as

$$\mathcal{L}_{fr} = -\text{MI}(F_t(x_t^j)_{j=1}^{B'}, \{p_j\}_{j=1}^{B'}). \quad (2)$$

As shown in Fig. 1, when the target model’s previous prediction for an image is confident, the current prediction interacts with both the corresponding ViL model prediction and the probability stored in the memory bank. Otherwise, it interacts only with the ViL model prediction. \mathcal{L}_{dis} and \mathcal{L}_{fr} together constitute a dual mutual information loss, formalizing the joint consideration of the ViL model’s knowledge and the target model’s past confident predictions within a mutual-information-based adaptation framework.

The reasons for also adopting mutual information as the forgetting-resistant loss are two-fold. First, mutual information considers the joint distributions of the current target model predictions and the stored previous predictions when preserving the target model’s reliable predictions. Second, such a loss choice makes it needless to balance the \mathcal{L}_{dis} and \mathcal{L}_{fr} with a hyperparameter, since they have the same scale. Thus, the final loss for the image-level supervision is

$$\mathcal{L}_{im} = \mathcal{L}_{dis} + \mathcal{L}_{fr}. \quad (3)$$

2.2 Lesion-Aware Adaptation with Adaptive Patch-level Supervision

Prior SFDA research which leverages foundation models only takes advantage of the global image information offered by foundation models, such as image-level probabilities [19] and image features [28], thus overlooking the more detailed

knowledge which is readily available from foundation models. We propose a lesion-aware adaptation module to utilize such fine-grained information, which contributes to making the target model aware of the lesion regions in fundus images. Specifically, we develop an adaptive patch-level supervision strategy that simultaneously takes into consideration the compatibility with reliable predictions in the memory bank, the class imbalance of patches, and the distraction from the primary learning objective.

Denote the feature of the vision branch of the ViL model [17] before the global average pooling (GAP) layer as $f_v \in \mathbb{R}^{B \times H \times W \times D_v}$ (H and W are the height and width of the feature map), the linear layer after the GAP layer as $\text{Linear}_{D \times D_v}(\cdot)$, and text features as $C \in \mathbb{R}^{K \times D}$ (both D_v and D are feature dimensions). Then the patch-wise predicted probabilities of the ViL model can be obtained in a manner similar to CAM [30] as

$$p_{v,p} = \text{softmax}\left(\frac{\text{Linear}(f_v)}{\text{norm}(\text{avg}(\text{Linear}(f_v)))} C^T\right) \in \mathbb{R}^{B \times H \times W \times K}, \quad (4)$$

where $\text{avg}(\cdot)$ averages the features along the height and width dimensions, $\text{norm}(\cdot)$ computes feature’s Euclidean norm, softmax operation is performed along the class dimension, and $p_{v,p}$ stands for the patch-wise probabilities predicted by the ViL model. In Eq. 4, the scaling parameter is omitted for simplicity. The patch-wise probabilities of the target model can be calculated likewise but without the division by the norm, since the target model itself does not normalize features.

Those ViL model’s patch-level probabilities whose labels are inconsistent with the confident image-level predictions in the memory bank in Sec. 2.1 are removed, since they are very likely to be wrong predictions, leading to new patch-level predictions $p'_{v,p} \in \mathbb{R}^{l \times K}$, with $l < B \times H \times W$.

Considering the potential patch class imbalance, the $p'_{v,p}$ is further rectified with class weights before being sent for the calculation of mutual information loss. Specifically,

$$p^r_{v,p,i} = p'_{v,p,i} / \sum_{j=1}^l \mathbb{1}(\text{argmax}(p'_{v,p,i}) = \text{argmax}(p'_{v,p,j})), \quad (5)$$

where $p^r_{v,p,i}$ signifies the i -th patch’s rectified probability predicted by the ViL model, $\mathbb{1}(\cdot)$ is the indicator function, and $\text{argmax}(\cdot)$ obtains the pseudo-label of a probability vector. In this way, each patch probability is normalized by the number of patches with the same predicted label, preventing the target model from being biased towards a certain class. Note that Eq. 5 makes the sum of a probability vector not equal to 1. However, this makes no difference to the calculation of mutual information, because the estimated joint distribution will be normalized over a batch [6, 19].

Though adding patch-wise supervision helps the target model be aware of the lesion regions which is a key to diagnosis, such a patch classification task might distract the model from its principal learning task which is image diagnosis. Therefore, a gradually attenuating loss weight is utilized. Let I , I_{max} represent

the current iteration number and the maximum iteration number, respectively. The lesion-aware adaptation loss is defined as

$$\mathcal{L}_{la} = -\lambda_{la} \cdot \max\left(\frac{I_{max}}{2} - I, 0\right) \cdot \text{MI}(p_{t,p}, p_{v,p}^r). \quad (6)$$

Here $p_{t,p}$ is the patch probabilities predicted by the target model corresponding to the patches in $p_{v,p}^r$. The weight of the loss declines gradually from λ_{la} to 0 in the first half of the training, then maintains 0 afterwards to avoid distraction from the image diagnosis task.

The total training loss is the sum of the forgetting-resistant image-level loss and the lesion-aware patch-level loss, i.e.,

$$\mathcal{L} = \mathcal{L}_{im} + \mathcal{L}_{la}. \quad (7)$$

3 Experiments

Datasets. To evaluate our proposed FRLA approach for SFDA for fundus image diagnosis, we build two source and target domain pairs with three datasets: ODIR [1], FIVES [7], and VietAI [2]. The ODIR is set as the source domain data. FIVES and VietAI are set as the target domain data, which are not employed as the training sets of FLAIR [17], the ViL model we adopt, so that fair experimental results can be produced. For each source and target domain pair, the images of four shared categories are chosen for our experiments. As a result, the number of images involved in our experiments are 5031 images, 800 images, and 1363 images, for ODIR [1], FIVES [7], and VietAI [2], respectively.

Implementation Details and Evaluation Metrics. Following [12, 19], ResNet-50 is utilized as the backbone of the source/target model, and a bottleneck layer is inserted after the backbone. We adopt the batch size of 16, SGD optimizer with a learning rate of 1e-3 and momentum 0.9, and 15 training epochs on both target datasets. The threshold τ in Sec. 2.1 is set to 0.95 following [18]. The initial weight for the lesion-aware loss λ_{la} in Eq. 6 is set to 0.3. The memory bank in Sec. 2.1 is updated before each epoch. We use FLAIR [17] with ResNet-50 being the backbone of the vision encoder as the ViL model. All images are resized to the size of 512×512 , and zero-padding is applied to rectangular images to avoid distortions [17]. The augmentations we apply include random horizontal flip, random rotation of $[-5, 5]$ degrees, and zoom scaling in the range $[0.9, 1.1]$ [17]. All experiments are conducted with PyTorch on a single GPU of NVIDIA RTX 3090. Given the possible class imbalance of fundus image datasets, we adopt the average accuracy over classes for evaluating SFDA performance [12, 19].

Comparison with State-of-the-Arts. For comprehensive comparisons, we compare FRLA with two groups of existing top-performing methods in two adaptation scenarios, as shown in Table 1, where “**F**” means using foundation model. The first group includes directly using the source model in the target domain (denoted as “Source”), directly applying the ViL model (FLAIR [17]), and “Source+FLAIR” which averages the results of the source model and FLAIR.

Table 1. Comparison (%) with state-of-the-arts on two settings. “F” means using foundation model during adaptation. The best results are highlighted in bold, and the second-best are underlined.

Methods	F	Source: ODIR; Target: FIVES					Source: ODIR; Target: VietAI				
		Avg	N	ARMD	DR	GLC	Avg	N	MD	DR	GLC
Source	-	64.5	61.0	61.5	68.5	67.0	65.4	82.9	66.9	68.9	43.1
FLAIR [17]	✓	73.5	92.5	92.0	57.5	52.0	72.1	77.1	<u>89.0</u>	82.1	40.1
Source+FLAIR	✓	73.8	90.0	86.5	61.0	57.5	73.3	89.0	80.3	79.3	44.7
SHOT [12]	✗	72.1	79.0	87.0	51.0	71.5	67.7	68.2	76.6	55.2	71.0
COWA [9]	✗	70.4	79.0	78.5	59.0	65.0	75.4	<u>92.4</u>	79.3	61.3	68.8
Co-learn [28]	✓	75.3	97.0	89.0	60.5	54.5	76.0	99.2	74.9	<u>80.7</u>	49.2
DIFO [19]	✓	<u>78.6</u>	<u>96.5</u>	<u>94.0</u>	<u>62.5</u>	61.5	<u>78.4</u>	73.5	86.6	79.3	<u>74.0</u>
FRLA (ours)	✓	80.4	97.0	95.5	61.0	<u>68.0</u>	80.8	78.9	89.6	77.4	77.4

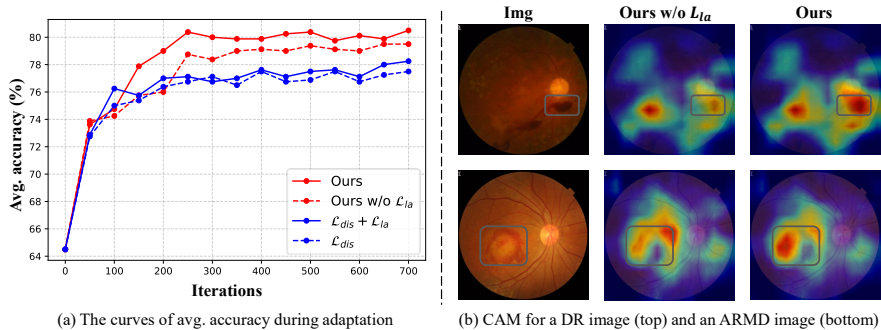
The second group comprises four state-of-the-art (SOTA) SFDA for classification methods: SHOT [12], COWA [9], Co-learn [28], and DIFO [19], where SHOT and COWA are traditional SFDA methods, and Co-learn, DIFO leverage foundation models. For a fair comparison, the vision encoder of FLAIR is adopted as the pre-trained network used in Co-learn. In Table 1, “N”, “ARMD”, “DR”, “GLC”, “MD”, and “Avg” stand for normal, age-related macular degeneration, diabetic retinopathy, glaucoma, macular degeneration, and average, respectively. The results indicate that our approach achieves clear improvements in average accuracy, over applying ViL model in a zero-shot manner, averaging the source model and ViL model predictions, as well as the SOTA SFDA methods. This is owing to our novel FRLA which mitigates negative model interaction found in mutual information loss supervision, and harnesses the rich fine-grained knowledge available from ViL model to guide the adaptation.

Ablation Study on Different Modules. Table 2 presents the ablation study for evaluating the contribution of each module in the two SFDA scenarios. Each component shows its critical role in enhancing the adaptation performance. Notably, introducing our forgetting-resistant adaptation (\mathcal{L}_{fr}) leads to a remarkable boost in average accuracy, underscoring its essential function in preventing the high-quality predictions of the target model from being forgotten. Similarly, incorporating the lesion-aware adaptation (\mathcal{L}_{la}) also results in a performance gain, as it enables the target model to acquire more informative patch-level guidance. Moreover, the integration of all components within the framework achieves the best performance, demonstrating their collective importance.

Effectiveness of Forgetting-Resistant Adaptation. The first two rows in Table 2 show that although the mutual information loss \mathcal{L}_{dis} brings about overall performance improvement, it can decrease the accuracy of the source model regarding a certain class, as reflected by the significant drop of the glaucoma accuracy on the ODIR-to-FIVES adaptation. Our forgetting-resistant adaptation maintains the well-predicted cases by the target model by forming another mutual information loss with a memory bank. On the ODIR-to-VietAI adaptation,

Table 2. Ablation study (%) on two adaptation settings. The first row is the accuracy of the source model.

\mathcal{L}_{dis}	\mathcal{L}_{fr}	\mathcal{L}_{la}	Source: ODIR; Target: FIVES				Source: ODIR; Target: VietAI					
			Avg	N	ARMD	DR	GLC	Avg	N	MD	DR	GLC
\times	\times	\times	64.5	61.0	61.5	68.5	67.0	65.4	82.9	66.9	68.9	43.1
\checkmark	\times	\times	77.3	98.0	94.0	62.0	55.0	77.5	76.0	85.6	73.1	75.2
\checkmark	\checkmark	\times	79.5	96.0	94.0	61.0	67.0	79.5	77.3	84.9	77.4	78.6
\checkmark	\times	\checkmark	78.3	98.0	94.5	62.0	58.5	79.0	77.0	85.6	80.2	73.4
\checkmark	\checkmark	\checkmark	80.4	97.0	95.5	61.0	68.0	80.8	78.9	89.6	77.4	77.4

**Fig. 2.** On the ODIR-to-FIVES adaptation: (a) The evolving dynamics of average accuracy during adaptation for different combinations of the losses. (b) The CAMs generated by the target models trained with our method and our method without \mathcal{L}_{la} . The gray boxes mark critical lesions recognized by a senior ophthalmologist.

introducing \mathcal{L}_{fr} leads to noticeable improvements in the accuracies of normal and glaucoma.

Effectiveness of Lesion-Aware Adaptation. Comparing the solid lines and corresponding dashed lines in Fig. 2 (a) indicates that \mathcal{L}_{la} helps target model learn better at early iterations, and eventually achieve a higher accuracy. We also give in Fig. 2 (b) the CAMs [30] when \mathcal{L}_{la} is utilized or not. The results show that \mathcal{L}_{la} enhances the model’s ability to recognize lesion regions, because of the detailed knowledge from the patch-wise interaction.

4 Conclusion

In this paper, we pinpoint and address two limitations in existing research on SFDA with foundation model. Specifically, we develop a forgetting-resistant adaptation module to explicitly protect the reliable predictions of the target model from being adversely affected by the ViL model. Besides, the proposed lesion-aware adaptation module produces fine-grained supervision, allowing the target model to better identify the lesion areas. Our experiments show that our method outperforms the state-of-the-art SFDA approaches.

References

1. International competition on ocular disease intelligent recognition. <https://odir2019.grand-challenge.org> (2019)
2. Vietai advance course - retinal disease detection. <https://www.kaggle.com/c/vietai-advance-retinal-disease-detection-2020/data> (2020)
3. Chen, C., Liu, Q., Jin, Y., Dou, Q., Heng, P.A.: Source-free domain adaptive fundus image segmentation with denoised pseudo-labeling. In: Proc. Int. Conf. Med. Image Comput. Comput.-Assist. Intervent. pp. 225–235. Springer (2021)
4. Chen, D., Wang, D., Darrell, T., Ebrahimi, S.: Contrastive test-time adaptation. In: Proc. IEEE Conf. Comput. Vis. Pattern Recognit. pp. 295–305 (2022)
5. Iqbal, S., Khan, T.M., Naveed, K., Naqvi, S.S., Nawaz, S.J.: Recent trends and advances in fundus image analysis: A review. *Computers in Biology and Medicine* **151**, 106277 (2022)
6. Ji, X., Henriques, J.F., Vedaldi, A.: Invariant information clustering for unsupervised image classification and segmentation. In: Proc. IEEE Int. Conf. Comput. Vis. pp. 9865–9874 (2019)
7. Jin, K., Huang, X., Zhou, J., Li, Y., Yan, Y., Sun, Y., Zhang, Q., Wang, Y., Ye, J.: Fives: A fundus image dataset for artificial intelligence based vessel segmentation. *Scientific data* **9**(1), 475 (2022)
8. Karim, N., Mithun, N.C., Rajvanshi, A., Chiu, H.p., Samarasekera, S., Rahnavard, N.: C-sfda: A curriculum learning aided self-training framework for efficient source free domain adaptation. In: Proc. IEEE Conf. Comput. Vis. Pattern Recognit. pp. 24120–24131 (2023)
9. Lee, J., Jung, D., Yim, J., Yoon, S.: Confidence score for source-free unsupervised domain adaptation. In: Proc. Int. Conf. Mach. Learn. pp. 12365–12377. PMLR (2022)
10. Li, J., Wang, H., Wang, W., Qin, J., Wang, Q., Zhu, L.: Source-free active domain adaptation for efficient medical video polyp segmentation. In: International Conference on Medical Image Computing and Computer-Assisted Intervention. pp. 499–509. Springer (2025)
11. Li, T., Bo, W., Hu, C., Kang, H., Liu, H., Wang, K., Fu, H.: Applications of deep learning in fundus images: A review. *Med. Image Anal.* **69**, 101971 (2021)
12. Liang, J., Hu, D., Feng, J.: Do we really need to access the source data? source hypothesis transfer for unsupervised domain adaptation. In: Proc. Int. Conf. Mach. Learn. pp. 6028–6039. PMLR (2020)
13. Liu, Z., Lin, Y., Cao, Y., Hu, H., Wei, Y., Zhang, Z., Lin, S., Guo, B.: Swin transformer: Hierarchical vision transformer using shifted windows. In: Proc. IEEE Int. Conf. Comput. Vis. pp. 10012–10022 (2021)
14. Ma, A., Zhu, Q., Li, J., Nielsen, M., Chen, X.: Source-free domain adaptation for cross-modality cardiac image segmentation with contrastive class relationship consistency. In: International Conference on Medical Image Computing and Computer-Assisted Intervention. pp. 574–583. Springer (2025)
15. Qu, S., Chen, G., Zhang, J., Li, Z., He, W., Tao, D.: Bmd: A general class-balanced multicentric dynamic prototype strategy for source-free domain adaptation. arXiv preprint arXiv:2204.02811 (2022)
16. Radford, A., Kim, J.W., Hallacy, C., Ramesh, A., Goh, G., Agarwal, S., Sastry, G., Askell, A., Mishkin, P., Clark, J., et al.: Learning transferable visual models from natural language supervision. In: Proc. Int. Conf. Mach. Learn. pp. 8748–8763. PMLR (2021)

17. Silva-Rodriguez, J., Chakor, H., Kobbi, R., Dolz, J., Ayed, I.B.: A foundation language-image model of the retina (flair): Encoding expert knowledge in text supervision. *Med. Image Anal.* **99**, 103357 (2025)
18. Sohn, K., Berthelot, D., Carlini, N., Zhang, Z., Zhang, H., Raffel, C.A., Cubuk, E.D., Kurakin, A., Li, C.L.: Fixmatch: Simplifying semi-supervised learning with consistency and confidence. *Proc. Adv. Neural Inf. Process. Syst.* **33**, 596–608 (2020)
19. Tang, S., Su, W., Ye, M., Zhu, X.: Source-free domain adaptation with frozen multimodal foundation model. In: *Proceedings of the IEEE/CVF Conference on Computer Vision and Pattern Recognition*. pp. 23711–23720 (2024)
20. Wang, L., Qi, C., Ou, C., An, L., Jin, M., Kong, X., Li, X.: Multieye: Dataset and benchmark for oct-enhanced retinal disease recognition from fundus images. *IEEE Trans. Med. Imaging* (2024)
21. Wang, S., Yu, L., Yang, X., Fu, C.W., Heng, P.A.: Patch-based output space adversarial learning for joint optic disc and cup segmentation. *IEEE Trans. Med. Imaging* **38**(11), 2485–2495 (2019)
22. Xu, Z., Lu, D., Wang, Y., Luo, J., Wei, D., Zheng, Y., Tong, R.K.y.: Denoising for relaxing: Unsupervised domain adaptive fundus image segmentation without source data. In: *Proc. Int. Conf. Med. Image Comput. Comput.-Assist. Intervent.* pp. 214–224. Springer (2022)
23. Yang, C., Guo, X., Chen, Z., Yuan, Y.: Source free domain adaptation for medical image segmentation with fourier style mining. *Med. Image Anal.* **79**, 102457 (2022)
24. Yang, J., Yu, X., Qiu, P., Marcus, D., Sotiras, A.: Active source-free cross-domain and cross-modality adaptation for volumetric medical image segmentation by image sensitivity and organ heterogeneity sampling. In: *International Conference on Medical Image Computing and Computer-Assisted Intervention*. pp. 3–12. Springer (2025)
25. Yang, S., Wang, Y., Wang, K., JUI, S., van de weijer, J.: Attracting and dispersing: A simple approach for source-free domain adaptation. In: Oh, A.H., Agarwal, A., Belgrave, D., Cho, K. (eds.) *Proc. Adv. Neural Inf. Process. Syst.* (2022)
26. Yang, S., van de Weijer, J., Herranz, L., Jui, S., et al.: Exploiting the intrinsic neighborhood structure for source-free domain adaptation. In: *Proc. Adv. Neural Inf. Process. Syst.* vol. 34, pp. 29393–29405 (2021)
27. Zhang, G., Qi, X., Yan, B., Wang, G.: Iplc: iterative pseudo label correction guided by sam for source-free domain adaptation in medical image segmentation. In: *Proc. Int. Conf. Med. Image Comput. Comput.-Assist. Intervent.* pp. 351–360. Springer (2024)
28. Zhang, W., Shen, L., Foo, C.S.: Rethinking the role of pre-trained networks in source-free domain adaptation. In: *Proc. IEEE Int. Conf. Comput. Vis.* pp. 18841–18851 (2023)
29. Zhang, Y., Wang, Z., He, W.: Class relationship embedded learning for source-free unsupervised domain adaptation. In: *Proc. IEEE Conf. Comput. Vis. Pattern Recognit.* pp. 7619–7629 (2023)
30. Zhou, B., Khosla, A., Lapedriza, A., Oliva, A., Torralba, A.: Learning deep features for discriminative localization. In: *Proc. IEEE Conf. Comput. Vis. Pattern Recognit.* pp. 2921–2929 (2016)
31. Zhou, Y., Bai, S., Zhou, T., Zhang, Y., Fu, H.: Delving into local features for open-set domain adaptation in fundus image analysis. In: *Proc. Int. Conf. Med. Image Comput. Comput.-Assist. Intervent.* pp. 682–692. Springer (2022)